

†Research supported in part by the U. S. Atomic Energy Commission and the National Science Foundation.

*Present address: Harvard College Observatory, Cambridge, Mass.

‡Alfred P. Sloan Fellow.

¹N. H. Deiter and W. M. Goss, *Rev. Mod. Phys.* **38**, 256 (1966).

²A. Dalgarno, *Rev. Mod. Phys.* **39**, 850 (1967).

³A. Dalgarno and M. R. H. Rudge, *Astrophys. J.* **140**, 800 (1964).

⁴J. Callaway and E. Bauer, *Phys. Rev.* **140**, A1072 (1965).

⁵F. J. Smith, *Planetary Space Sci.* **14**, 937 (1966).

⁶J. Callaway and A. F. Dugan, *Phys. Rev.* **163**, 162 (1967).

⁷F. J. Smith, *Monthly Notices Roy. Astron. Soc.* **140**, 341 (1968).

⁸S. Wofsy, R. H. G. Reid, and A. Dalgarno (unpublished).

⁹P. Moore, Ph. D. thesis [University of Texas (Austin), 1965] (unpublished).

¹⁰J. C. Browne (private communication).

¹¹N. F. Mott and H. S. W. Massey, *The Theory of Atomic Collisions*, 3rd ed. (Oxford U. P., London, 1965).

¹²A. Dalgarno and W. D. Davison, *Advances in Atomic and Molecular Physics* (Academic, New York, 1966), Vol. 2.

¹³L. Castellejo, J. C. Percival, and M. J. Seaton, *Proc. Roy. Soc. (London)* **A254**, 259 (1960).

¹⁴A. Dalgarno, G. W. F. Drake, and G. A. Victor, *Phys. Rev.* **176**, 194 (1968).

¹⁵J. C. Weishelt, Ph. D. thesis (Rice University, 1970) (unpublished).

¹⁶A. M. Arthurs and A. Dalgarno, *Proc. Roy. Soc. (London)* **A256**, 540 (1960).

¹⁷A. Dalgarno, *Proc. Roy. Soc. (London)* **A262**, 132 (1961).

¹⁸A. Dalgarno and M. R. H. Rudge, *Proc. Roy. Soc. (London)* **A286**, 519 (1965).

¹⁹M. E. Rose, *Elementary Theory of Angular Momentum* (Wiley, New York, 1957), Chap. IV.

²⁰N. F. Lane and S. Geltman, *Phys. Rev.* **160**, 53 (1967).

²¹D. C. S. Allison and P. G. Burke, *J. Phys.* **B2**, 941 (1969).

²²E. Clementi, *IBM J. Res. Develop. Suppl.* **9** (1965).

²³D. R. Hartree, *The Calculation of Atomic Structures* (Wiley, New York, 1957).

Electron Impact Excitation of the Rare Gases*

P. S. Ganas† and A. E. S. Green

University of Florida, Gainesville, Florida 32601

(Received 11 January 1971)

We utilize the analytic atomic independent-particle model (IPM) of Green, Sellin, and Zachor as a basis for calculating generalized oscillator strengths for the single-particle excitations of Ne, Ar, Kr, and Xe. First, we establish averages of the experimental energy levels to arrive at single-particle states. We then adjust the two parameters so that the IPM potentials accurately characterize these excited-state energies. Using the wave functions associated with these potentials and the Born approximation, we calculate the generalized oscillator strengths for excitations to p^5ns states. A very complex nodal structure is apparent at large values of momentum transfer and a rapid decline in magnitude occurs after the second node. We may accurately characterize the results up to the second node with a convenient analytic form which leads to analytic total excitation cross sections. We use available optical oscillator strengths to normalize our results. The systematics and regularities of the parameters for various Rydberg series are discussed and approximate scaling laws are given.

I. INTRODUCTION

In a series of studies,¹⁻⁵ simple two-parameter analytic independent-particle-model (IPM) potential has been found to provide a good representation of electron-atom interactions. The data used in adjusting these two parameters have been determined by experiment⁶ or by using the results of Hartree-Fock⁷ (HF) or Hartree-Fock-Slater⁸ (HFS) descriptions of the atom. In this work we explore further consequences of this simple realistic model by carrying out calculation of inelastic excitation cross sections for rare-gas atoms, giving particular concentration to systematic properties which

are needed for applied problems.

We deal primarily with the rare gases Ne, Ar, Kr, and Xe despite the fact that there is a scarcity of experimental data with which to test our results or to readjust our parameters in the potential. However, our work is approximately consistent with the available experiment and the attempts to utilize the few available HF excited-state wave functions. It is hoped, therefore, that this work, which covers a greater number of cases and a far more extended range of momentum transfer, might provide a guideline which will stimulate further measurements on rare-gas excitation cross sections and more rigorous calculations. These are needed not

only to test this approach, which uses plane waves for the incident and outgoing electrons, but also to test calculations which we have underway at lower energies using distorted waves.

II. EXPERIMENTAL LEVELS

The ground state of each rare-gas atom is a p^6 configuration with all lower-energy shells filled. The known excited states of these atoms have p^5 cores; i. e., they correspond to configurations like p^5ns , p^5np , p^5nd , . . . , where one electron is excited. The spectra of the rare-gas atoms exhibit considerable fine structure as shown in the tables of Moore.⁹ This arises from the variety of possibilities which occur when the angular momentum of the core J_c is coupled to the angular momentum of the excited electron j to give a total angular momentum J . The core angular momentum J_c takes the values $\frac{3}{2}$ and $\frac{1}{2}$. When $J_c = \frac{3}{2}$, the orbital angular momentum of the excited electron is designated by s , p , d , f , and when $J_c = \frac{1}{2}$, by s' , p' , d' , and f' .

To simplify the analysis of the rare-gas spectra we replace each multiplet by a center of gravity by averaging over J :

$$E_{nl} = \sum_J (2J+1) \bar{E}_{nlJ} / \sum_J (2J+1), \quad (1)$$

where all energies are converted to atomic units ($R=1$ Ry). Here, n and l are the principal quantum number and orbital angular momentum, respectively, of the excited state and \bar{E}_{nlJ} is the energy of the configuration p^5nl when the total angular momentum is equal to J . We treat configurations associated with $J_c = \frac{3}{2}$ separately from configurations associated with $J_c = \frac{1}{2}$. In other words, for each configuration p^5nl we perform two separate averages; one corresponds to $J_c = \frac{3}{2}$ and the other to $J_c = \frac{1}{2}$. To illustrate with an example, let us consider the $3p^54s$ configuration in Ar. Corresponding to $J_c = \frac{3}{2}$, there is a $J=1$ level at -0.3040 Ry and a $J=2$ level at -0.3095 Ry; the center of gravity, calculated from Eq. (1), is a $4s$ state lying at -0.3074 Ry. On the other hand, when $J_c = \frac{1}{2}$, there is a $J=0$ level at -0.2967 Ry and a $J=1$ at -0.2890 Ry; the center of gravity is a $4s'$ state lying at -0.2909 Ry. In this manner we reduce Moore's tabulated spectra to two sets of single-particle states for each gas. These results are displayed as solid lines in Figs. 1-4.

The s , p , d , f states tend to a different ionization limit from the s' , p' , d' , f' states. However, we have found that to a good approximation any state nl differs from the corresponding state nl' by a constant energy ΔI , where ΔI is the difference between the two ionization limits. This has the useful consequence that the wave functions for corresponding states nl and nl' are very nearly equal. Because of the close relationships between the s , p , d , f and s' , p' , d' , f' systems just noted, we have

combined the two systems into a final average which we obtain thus: We subtract ΔI from all of the energies of the s' , p' , d' , f' system and then combine these energies with the corresponding ones from s , p , d , f system in the ratio $\frac{1}{3}:\frac{2}{3}$. These final averages serve as our experimental single-particle energy levels. These levels conform quite well to a Rydberg-series formula. In Table I, we present the quantum defects for the rare gases as deduced from these experimental single-particle energies. The quantum defect δ is defined by

$$E_{nl} = -(n - \delta)^{-2} \quad (\text{in Ry}). \quad (2)$$

Thus to generate the higher s , p , d , f single-particle energy levels, we may use Eq. (2). To generate the s' , p' , d' , f' single-particle energy levels we add ΔI .

III. IPM POTENTIAL

The potential for an electron in a neutral atom may be written as (in a. u.)

$$V(r) = -2r^{-1} [(Z-1)\Omega(r)+1], \quad (3)$$

where $\Omega(r)$ is a screening function. In the present work $\Omega(r)$ is chosen to have the form used by Green, Sellin, and Zachor¹ (GSZ):

$$\Omega(r) = [H(e^{r/d} - 1) + 1]^{-1}. \quad (4)$$

Here d and H are phenomenological parameters. We insert the potential into the radial Schrödinger equation

$$\left(\frac{d^2}{dr^2} - \frac{l(l+1)}{r^2} - V(r) + E_{nl} \right) P_{nl}(r) = 0 \quad (5)$$

and obtain the energy eigenvalues and wave functions using a subprogram of the Herman and Skillman HFS computer code.⁸ In practice we couple this subprogram to a nonlinear least-squares automatic search subroutine; this enables us to vary the parameter d and H so as to obtain good fits to the experimental single-particle energies. We performed two kinds of searches. (a) For each gas we searched over the bound plus the excited states. The best fits in this case are denoted by the symbol \square in Figs. 1-4, and the best-fit parameters are given in Table II. (b) For each gas we also searched over the excited states only, including the ground state but not the inner states. The best fits in this case are denoted by the symbol \odot in Figs. 1-4, and the best-fit parameters are given in Table II. In all our searches, the data points were weighted as the inverse of the experimental values. Also included in Table II are the values obtained by GSZ, who searched over the bound states only. It is evident that the best parameters from the three kinds of search vary somewhat.

In the work which follows we calculate generalized oscillator strengths and total cross sections for

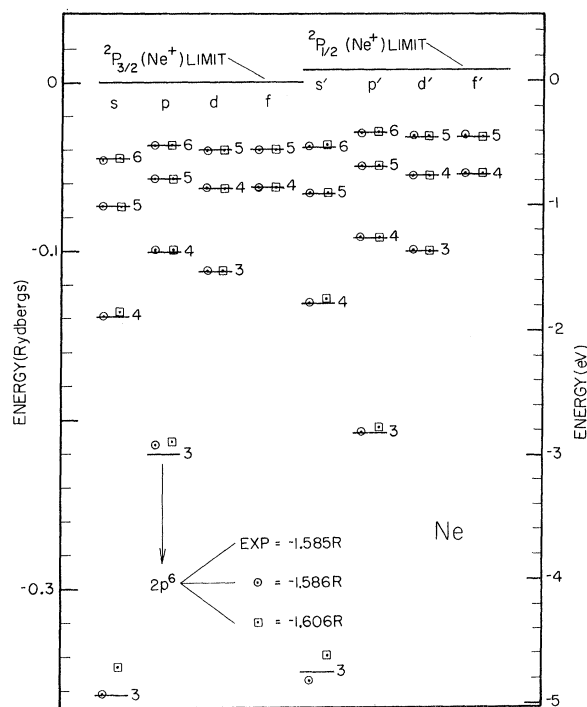


FIG. 1. Excited-state energies of neon. The lines denote average of experimental levels. The position of the ground state is indicated by numerical values. The symbols \circ and \square denote theoretical IPM energy levels based upon corresponding parameters in Table II.

transitions from the ground state to the excited states. We use the parameters from search (b) above, since this search yields somewhat more precise fits to the excited states than do the other searches.

IV. MATHEMATICAL DESCRIPTION

We consider the transition of an N -electron atom from its ground state to the n th excited state with momentum transfer K . We define

$$x = K^2 a_0^2, \quad (6)$$

where a_0 is the Bohr radius, and

$$x_t = (E_n - E_0)/R = W/R, \quad (7)$$

where E_n is the excitation energy of the n th state, E_0 is the ground-state energy, and R is the Rydberg

TABLE I. Quantum defects and ionization-limit differences (units of ΔI are rydbergs).

	s	p	d	f	ΔI
Ne	1.33	0.86	0.014	0.000	0.0071
Ar	2.19	1.73	0.212	0.010	0.0130
Kr	3.16	2.68	1.27	0.008	0.0489
Xe	4.11	3.61	2.42	0.025	0.0960

TABLE II. IPM potential parameters.

		\circ	\square	GSZ
Ne	d	0.715	0.465	0.500
	H	2.219	1.130	1.204
Ar	d	0.997	0.776	0.862
	H	3.469	2.462	2.677
Kr	d	1.055	0.617	0.689
	H	5.507	2.532	2.857
Xe	d	1.175	0.684	0.940
	H	6.805	3.109	4.600

energy. We shall also make considerable use of the reduced or scaled quantity

$$\xi = x/x_t = K^2 a_0^2 R/W. \quad (8)$$

Our primary results depend upon the evaluation of matrix elements given by¹⁰⁻¹²

$$I = \sum_{j=1}^N \int \psi_n^* e^{i\vec{k}\cdot\vec{r}_j} \psi_0 d\vec{r}_1 \cdots d\vec{r}_N. \quad (9)$$

Here \vec{r}_j is the position of the j th electron, and ψ_N and ψ_0 are the excited-state and ground-state wave functions, respectively, of the atom. Let us suppose that only one electron is involved in the transition, the core remaining undisturbed. Suppose the electron is promoted from its ground state with quantum numbers $n_0, l_0,$ and m_0 to an excited state with quantum numbers $n, l,$ and m . Here n_0 and

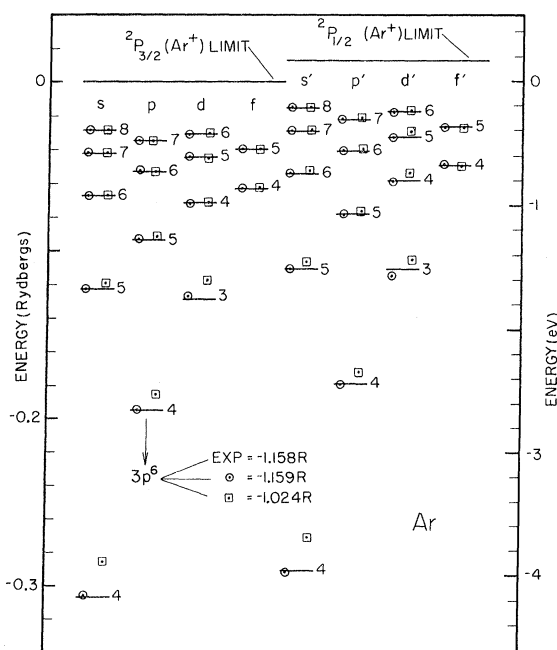


FIG. 2. Excited-state energies of argon (see caption to Fig. 1).

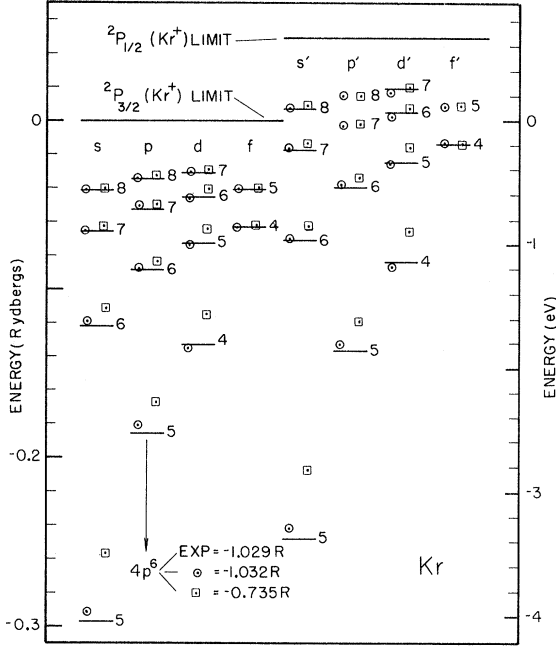


FIG. 3. Excited-state energies of krypton (see caption to Fig. 1).

n are the principal quantum numbers for the ground and excited states, respectively, l_0 and l are the angular momentum quantum numbers, and m_0 and m are the magnetic quantum numbers. Then, under

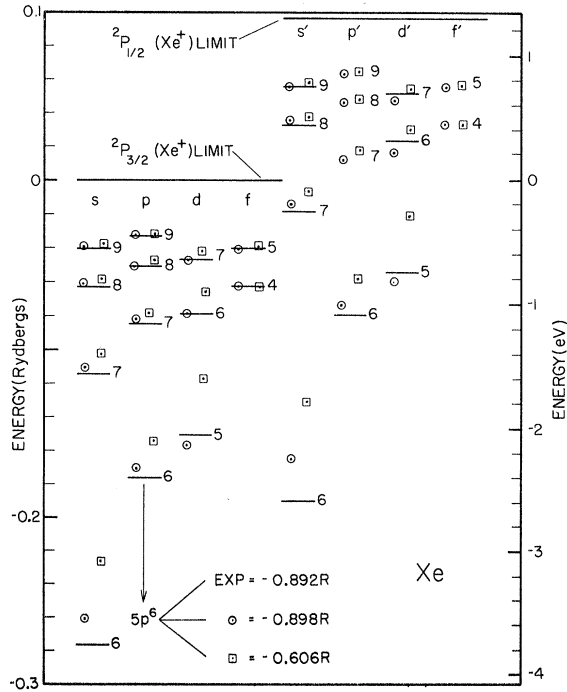


FIG. 4. Excited-state energies of xenon (see caption to Fig. 1).

these conditions the matrix element I simplifies to $I = C\mathcal{I}$, where

$$\mathcal{I} = \int \psi_{n_0 l_0 m_0}^*(\vec{r}) e^{i\vec{k}\cdot\vec{r}} \psi_{n l m}(\vec{r}) d\vec{r}. \quad (10)$$

Here C is a normalization constant which, in the present treatment, will be determined phenomenologically. A full physical and mathematical treatment of the problem would entail considerable use of the algebra of angular momentum couplings. Furthermore, it is known that the results depend on what kind of an angular momentum coupling scheme is used; it is also known that light, intermediate, and heavy atoms are subject to different coupling schemes. The introduction of a phenomenological normalization constant circumvents these complications and simplifies the formal treatment of the problem without losing the essential features which involve the determination of radial matrix elements.

In order to evaluate the integral in Eq. (10), we first separate the wave functions into their radial and angular parts:

$$\psi_{n_0 l_0 m_0}(\vec{r}) = R_{n_0 l_0}(r) Y_{l_0 m_0}(\theta, \phi), \quad (11a)$$

$$\psi_{n l m}(\vec{r}) = R_{n l}(r) Y_{l m}(\theta, \phi). \quad (11b)$$

Then, making use of the Rayleigh expansion

$$e^{i\vec{k}\cdot\vec{r}} = \sum_{l'=0}^{\infty} B_{l'} j_{l'}(Kr) Y_{l' 0}(\theta, \phi), \quad (12)$$

where

$$B_l = i^l (4\pi)^{1/2} (2l+1)^{1/2} \quad (13)$$

and $j_l(Kr)$ is a spherical Bessel function, and using the spherical harmonic property

$$\int Y_{a\alpha} Y_{b\beta} Y_{c\gamma} \sin\theta d\theta d\phi = \left[\frac{(2a+1)(2b+1)(2c+1)}{4\pi} \right]^{1/2} \begin{pmatrix} a & b & c \\ \alpha & \beta & \gamma \end{pmatrix} \begin{pmatrix} a & b & c \\ 0 & 0 & 0 \end{pmatrix},$$

TABLE III. Angular factors $A(r)$ given by Eq. (15) for various transitions in the rare gases.

I	$p \rightarrow s$ transitions $n_0, 1, 0 \rightarrow n, 0, 0$	$i\sqrt{3} j_1(Kr)$
II	$p \rightarrow p$ transitions (a) $n_0, 1, 0 \rightarrow n, 1, 0$ (b) $n_0, 1, \pm 1 \rightarrow n, 1, \pm 1$	$j_0(Kr) - 2j_2(Kr)$ $j_0(Kr) + j_2(Kr)$
III	$p \rightarrow d$ transitions (a) $n_0, 1, 0 \rightarrow n, 2, 0$ (b) $n_0, 1, \pm 1 \rightarrow n, 2, \pm 1$	$(i\sqrt{15}/5)[2j_1(Kr) - 3j_3(Kr)]$ $(i\sqrt{5}/5)[3j_1(Kr) + 3j_3(Kr)]$
IV	$p \rightarrow f$ transitions (a) $n_0, 1, 0 \rightarrow n, 3, 0$ (b) $n_0, 1, \pm 1 \rightarrow n, 3, \pm 1$	$(-\sqrt{21}/7)[3j_2(Kr) - 4j_4(Kr)]$ $(-3\sqrt{14}/7)[j_2(Kr) + j_4(Kr)]$

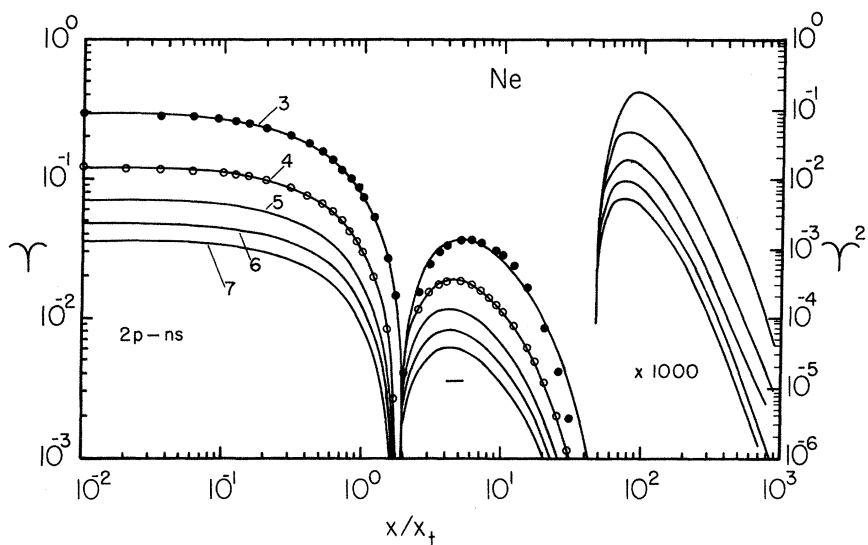


FIG. 5. Curves indicating reduced oscillator amplitude (left scale) and oscillator strengths (right scale) for neon versus reduced square of momentum transfer. The solid dots give a representative analytic fit using three adjustable parameters. The open circles give a representative fit using only one adjustable parameter.

where the arrays in brackets are $3j$ symbols, it is easy to show that

$$g = \int_0^\infty R_{n_0 l_0}(r) A(r) R_{nl}(r) r^2 dr, \quad (14)$$

where

$$A(r) = (-)^{m_0} [(2l_0 + 1)(2l + 1)]^{1/2} \sum_{l'} i^{l'} (2l' + 1) \times \begin{pmatrix} l_0 & l & l' \\ -m_0 & m & 0 \end{pmatrix} \begin{pmatrix} l_0 & l & l' \\ 0 & 0 & 0 \end{pmatrix} j_{l'}(Kr). \quad (15)$$

The summation index l' runs from $|l - l_0|$ to $l + l_0$ in steps of two units. From a property of the $3j$ symbol it follows that the magnetic quantum number is conserved: $m = m_0$. The expression (15) for the angular factor $A(r)$ holds for a general transition

$(n_0 l_0 m_0) \rightarrow (nlm)$. In Table III we evaluate the angular factor for various transitions in the rare gases. It may be noted that our results in Table III are consistent with those of Bonham.¹³

To apply our results we make use of the so-called generalized oscillator strength which is defined by

$$f(x) = \sum_{m_0 m} \frac{|I|^2}{\xi}. \quad (16)$$

This quantity, which goes over to the usual optical oscillator strength as $x \rightarrow 0$, may be used to give the differential and total excitation cross sections.

For allowed transitions such as $p-s$ and $p-d$ it is also convenient to introduce the reduced radial matrix element defined by

$$S_{l'}(\xi) = \xi^{-1/2} \int_0^\infty R_{n_0 l_0}(r) j_{l'}(Kr) R_{nl}(r) r^2 dr. \quad (17)$$

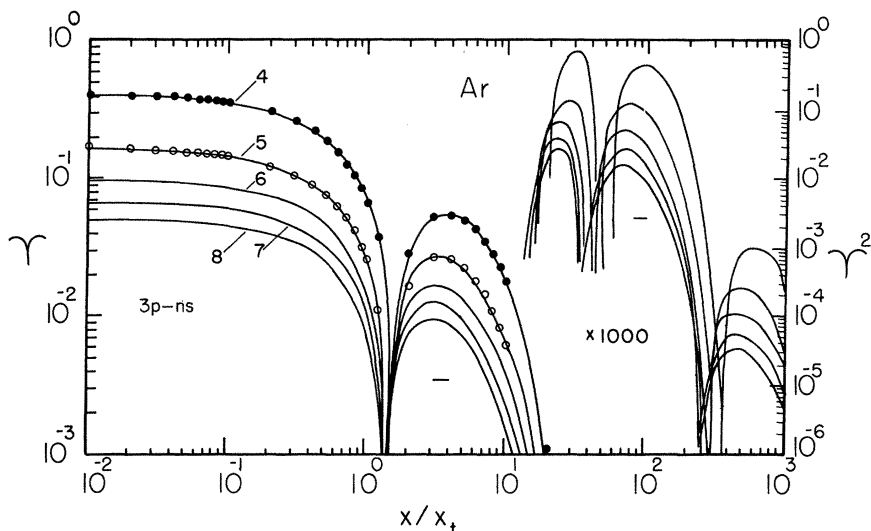


FIG. 6. Curves for argon (see caption to Fig. 5).

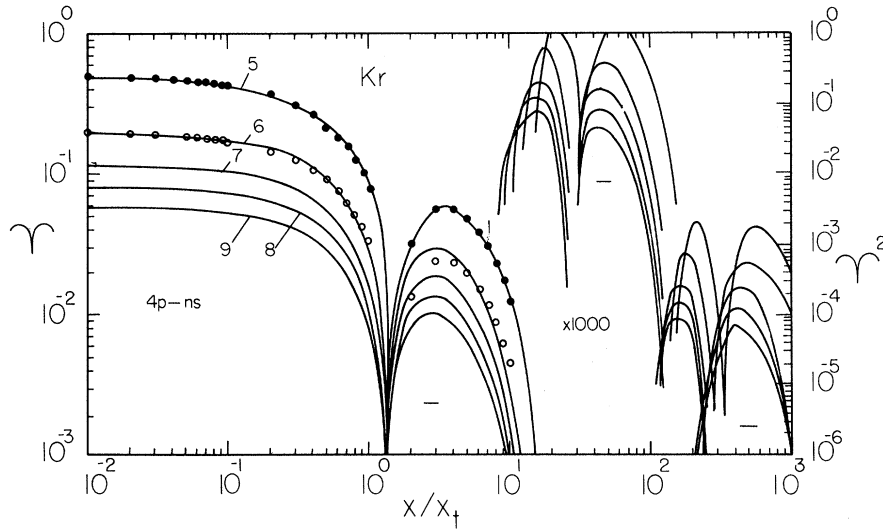


FIG. 7. Curves for krypton (see caption to Fig. 5).

From Eqs. (14)–(16) it may be shown that

$$f(x) = C^2 \sum_{l'} (2l_0 + 1)(2l + 1)(2l' + 1) \begin{pmatrix} l_0 & l & l' \\ 0 & 0 & 0 \end{pmatrix} S_{l'}^2, \quad (18)$$

where in this work the constant C is determined by using the fact that $f(x)$ goes over to the optical oscillator strength in the limit $x \rightarrow 0$. Clearly the essence of any systematic behavior of generalized oscillator strengths depends upon the properties of such reduced radial matrix elements as $S_{l'}(\xi)$. In Sec. IV we use our IPM descriptions to determine how this function behaves for the various p - s Rydberg series in rare gases.

V. RELATIVE OSCILLATOR AMPLITUDES AND STRENGTHS FOR p - ns TRANSITIONS

The results of our calculation for $\Upsilon = \sqrt{3} S_1(\xi)$ (left scale) and Υ^2 (right scale) for $2p$ - ns excita-

tions in Ne, $3p$ - ns in Ar, $4p$ - ns in Kr, and $5p$ - ns in Xe are shown in Figs. 5–8. Log-log paper is used to cover a large range of ξ and Υ and to further save space, Υ values beyond the second node are multiplied by 10^3 (10^2 for Xe). The negative signs between the nodes (to be denoted by ξ_1, ξ_2 , etc.) denote regions of negative Υ values which lie between ξ_1 and ξ_2 ; ξ_3 and ξ_4 ; ξ_5 and ξ_6 ; etc. Concentrating momentarily on neon (Fig. 5), we note that the regularities in the amplitudes for these Rydberg series when presented as a function of the reduced variable $\xi = a_0^2 K^2 R/W$ are indeed remarkable. A foretaste of such a regularity was noted earlier by Green and Dutta¹² for helium transitions. However, their calculations involved results with much simpler structure, and covered a far more restricted range of ξ .

Similar regularities are seen in the five transi-

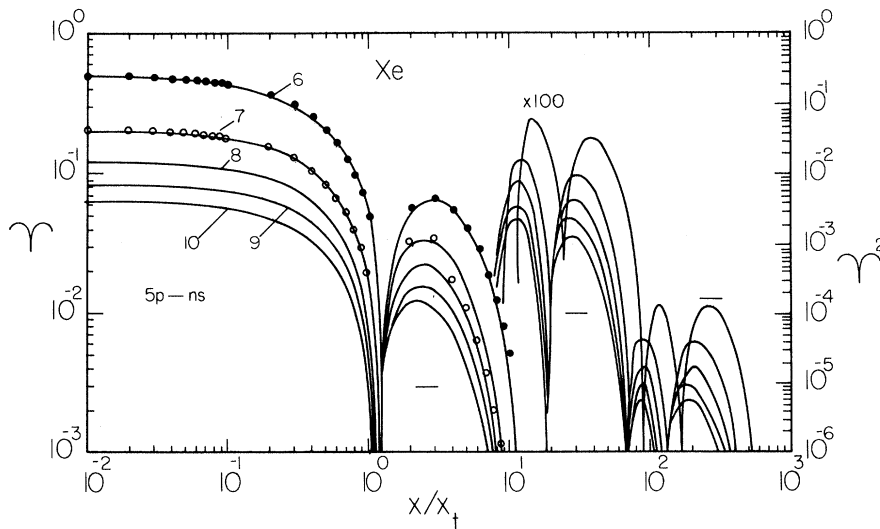


FIG. 8. Curves for xenon (see caption to Fig. 5).

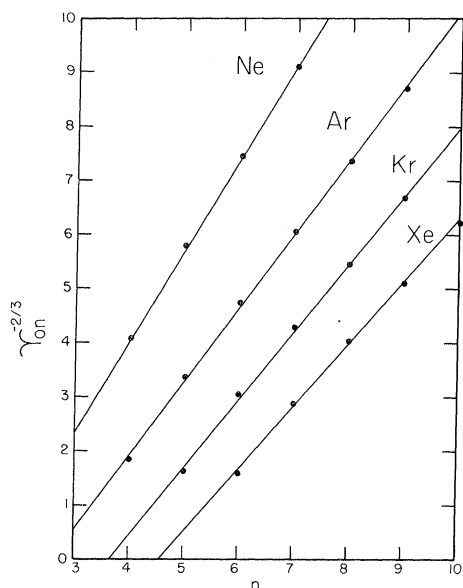


FIG. 9. Functions $\gamma_{0n}^{-2/3}$ vs n for $n_0p - ns$ transitions, illustrating validity of Eq. (19).

tions for argon shown in Fig. 6, particularly with respect to the region $\xi < 20$. At large ξ values the nodal structure becomes more complex and the ξ values of the nodes separate in a fashion which shows some systematic behavior.

Similar regularities and systematics occur in krypton (Fig. 7), which has a still more complicated nodal structure beyond $\xi > 15$. For xenon (Fig. 8) the second node moves further inward to $\xi \sim 10$ and separation again occurs. The results at still larger values of ξ are even more complex, although systematic behavior is again apparent.

VI. PHENOMENOLOGICAL REPRESENTATION OF RESULTS

Clearly the diagrams in the previous section illustrate the massive quantity of information which is potentially available from our calculations. Let us consider now how we may compact this information and present it in quantitative form which may be useful in applications.

Let us first consider the values of $\Upsilon(0)$, since $\Upsilon^2(0)$ should measure the relative optical oscillator strengths in Rydberg series. Previously Green

TABLE IV. Quantum defects and relative optical oscillator strength constants for $n_0p - ns$ transitions.

	δ	Υ_0^*	Υ_0^{*2}
Ne	1.62	0.453	0.205
Ar	2.57	0.630	0.396
Kr	3.63	0.716	0.512
Xe	4.57	0.804	0.647

and Dutta,¹² based upon their helium studies, proposed the rule

$$f_n = f^*/(n - \delta)^3. \quad (19)$$

A similar rule has been suggested by Fano and Cooper.¹⁴ Equation (19) suggests, of course, that $\Upsilon_{0n} = \Upsilon_0^*(n - \delta)^{-3/2}$. In Fig. 9, we show the values of $\Upsilon_{0n}^{-2/3}$ vs n . These follow straight lines rather well, thus confirming Eq. (19). The values of Υ_0^* and δ for the δ for the various gases as determined by least-squares fits are given in Table IV. Note that the quantum defects obtained differ from those used to characterize the energies of the s states in the transition as given in Table I. This might have been expected since, of course, the quantum defects of the ground states are also involved.

While the behavior of Υ in Figs. 5–8 beyond ξ_2 is quite complicated, the behavior for $\xi < \xi_2$ is fairly simple. Since there is a rapid falloff in each case beyond ξ_2 , we shall tentatively ignore this domain and simply seek a convenient quantitative representation of $\Upsilon(\xi)$ and hence $f(\xi)$ within ξ_2 . We have had good success with the representation

$$\Upsilon(\xi) = \Upsilon_0(e^{-\gamma_0\xi} - \kappa\xi e^{-\gamma_1\xi}). \quad (20)$$

The dots shown on the $2p-3s$ curve for Ne, $3p-4s$ for Ar, $4p-5s$ for Kr, and $5p-6s$ for Xe in Figs. 5–8 are examples of the fits within ξ_2 which can be achieved by fitting γ_0 , κ , and γ_1 to the results of our calculations. The values of the parameters for various Rydberg series obtained by use of a non-linear least-square program are given in successive rows in Table V. Also given are $100\chi^2$ obtained when the weight $1/\Upsilon$ is used for each point. The columns are headed by the gas, the ground-state designation, and the ground-state energy according

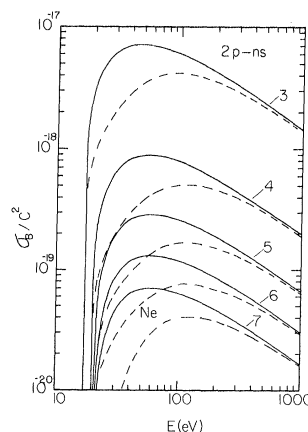


FIG. 10. Reduced cross sections for neon. The solid curve is based upon our representation of Born generalized oscillator strength. The dashed curves illustrate distortion effects based upon Eq. (27).

TABLE V. Parameters for analytic amplitudes.

Ne (2p 1.585)				Ar (3p 1.158)				Kr (4p 1.029)				Xe (5p 0.891)			
	(3)	(1)	(0)		(3)	(1)	(0)		(3)	(1)	(0)		(3)	(1)	(0)
3s	1.22	1.25	1.25	4s	1.35	1.25	1.25	5s	1.35	1.25	1.25	6s	1.42	1.25	1.25
0.360	0.063	0.063	0.065	0.306	0.137	0.182	0.182	0.297	0.152	0.173	0.180	0.280	0.253	0.417	0.40
1.225	0.190	0.210	0.20	0.852	0.346	0.400	0.400	0.732	0.408	0.42	0.436	0.611	0.553	0.725	0.725
0.303	0.98	1.74	1.94	0.400	0.80	1.47	2.00	0.476	1.30	1.56	1.59	0.507	1.62	3.51	3.58
4s	1.16			5s	1.18			6s	1.12			7s	0.849		
0.139	0.100	0.082		0.124	0.240	0.204		0.120	0.310	0.186		0.121	0.735	0.459	
1.446	2.32			1.035	0.429			0.909	0.530			0.771	0.765		
0.125	0.90	1.09	1.71	0.166	0.82	0.89	0.91	0.190	0.98	2.01	1.90	0.210	1.89	1.86	2.51
5s	1.14			6s	1.13			7s	1.02			8s	0.420		
0.074	0.114	0.086		0.067	0.277	0.209		0.066	0.398	0.186		0.064	1.17	0.393	
1.512	0.245			1.091	0.453			0.963	0.575			0.828	0.684		
0.074	0.78	1.00	1.74	0.100	0.71	0.89	0.94	0.115	0.84	2.01	1.89	0.129	1.00	4.83	4.83
6s	1.13			7s	1.11			8s	0.954			9s	0.823		
0.045	0.120	0.089		0.042	0.295	0.210		0.042	0.454	0.185		0.040	0.791	0.479	
1.540	0.251			1.116	0.463			0.987	0.598			0.851	0.781		
0.051	0.69	0.89	1.68	0.069	0.63	0.85	0.88	0.079	0.74	1.85	1.80	0.091	1.89	1.70	2.32
7s	1.13			8s	1.10			9s	0.655			10s	0.411		
0.081	0.124	0.090		0.029	0.306	0.212		0.029	0.738	0.178		0.029	1.23	0.508	
1.554	0.254			1.129	0.469			1.000	0.652			0.863	0.687		
0.038	0.61	0.80	1.61	0.052	0.56	0.90	0.80	0.060	0.95	3.45	3.45	0.067	0.83	1.41	7.50

to the IPM potential characterized by the parameters in the second column of Table II. The four rows of the first column in each block give the excited-state designation, its energy value, the transition energy, and the optical amplitude Υ_0 . The values of γ_0 , κ , γ_1 , and $100\chi^2$ for three-parameter searches are given in the second set of columns. After making these searches we noted that $\gamma_0 \sim 1.25$ in almost all cases. Furthermore, for each rare gas γ_1 did not vary very greatly. Accordingly, since there is usually ambiguity in three-parameter fitting, we conducted a restricted search on κ alone using the fixed decay lengths γ_0 , γ_1 , and the Υ_0 previously obtained. The results are given in the third set of columns in Table V with the fixed parameters γ_0 and γ_1 given only in the upper block. In the fourth sets of columns we give the results for all parameters fixed. In effect this case implies fixed shapes for the generalized oscillator strengths of a Rydberg series when using the reduced variable $\xi = a_0^2 K^2 R/W$. From the increases in χ^2 one sees that these results are not quite as good as the three-parameter results. However, they are still quite good. The dots in relation to the curves for second excited states in Figs. 5-8 are illustrative of fixed shape fits.

VII. CROSS SECTIONS

The practical aspects of our study of generalized oscillator strengths arise from its usefulness in providing cross sections. Thus the differential cross section can be expressed as¹²

$$\frac{d\sigma}{d\Omega} = \frac{q_0}{\pi W^2} \left(1 - \frac{W}{E}\right)^{1/2} \frac{f(\xi)}{\xi}, \quad (21)$$

where $q_0 = 4\pi a_0^2 R^2$. We may translate ξ into angles using

$$\xi = \frac{2E}{W} \left[1 - \cos\theta \left(1 - \frac{W}{E}\right)^{1/2} - \frac{W}{2E}\right]. \quad (22)$$

The total cross section is given by

$$\sigma = \frac{q_0}{WE} \int_{\xi_1}^{\xi_u} \frac{f(\xi)}{\xi} d\xi, \quad (23)$$

where for ξ_1 , forward scattering, $\cos\theta = 1$, and for ξ_u , backward scattering, $\cos\theta = -1$. When expressing W and E in eV and cross sections in cm^2 , $q_0 = 6.514 \times 10^{-14} \text{ cm}^2 \text{ eV}^2$. For $E \gg W$, $\xi_u \approx 4E/W$ and $\xi_1 \approx W/4E$. Thus for typical bombarding energies for which the Born approximation is valid we make use of a large part of the range of ξ given in Figs. 5-8.

The rapid decline of $f(\xi)$ after the second node together with the weighting by ξ^{-1} in Eqs. (21) and (23) minimizes the errors associated with our approximate analytic representation [Eq. (20)]. Now we see the main advantage of this approximate analytic representation for Υ in that it gives an approximate representation of f in the form of Green and Dutta,¹²

$$f(\xi) = \sum_s f_s \xi^s e^{-\alpha_s \xi}. \quad (24)$$

The total cross section corresponding to this equation is analytically integrable and is given by

$$\sigma(E) = \frac{q_0}{WE} \left(f_0 [E_1(\alpha_0 \xi_l) - E_1(\alpha_0 \xi_u)] + \sum_{s=1}^{\infty} \frac{f_s}{\alpha_s^2} [\gamma(s, \alpha_s \xi_u) - \gamma(s, \alpha_s \xi_l)] \right), \quad (25)$$

where E_1 is the first exponential integral and $\gamma(s, y)$ is the incomplete γ function.¹⁵ The first term in this series which is dominant at high energies leads to the familiar $E^{-1} \ln E$ dependence usually associated with the Born approximation.

Because of our success in Sec. VI in fitting $\Upsilon(\xi)$ with Eq. (20), we may use Eq. (24) simply by identifying

$$\begin{aligned} f_0 &= C^2 \Upsilon_0^2, & f_1 &= -2C^2 \Upsilon_0^2 \kappa, & f_2 &= C^2 \Upsilon_0^2 \kappa^2, \\ \alpha_0 &= 2\gamma_0, & \alpha_1 &= \gamma_0 + \gamma_1, & \alpha_2 &= 2\gamma_1. \end{aligned} \quad (26)$$

The results of relative ($C^2 = 1$) total cross sections for Rydberg series generated by this approach are shown in Figs. 10–13.

The dotted curves in Figs. 10–13 are based upon a distorted generalized oscillator strength (DGOS) of Green and Dutta¹² given by

$$f_d(\xi, E) = \left(1 - \frac{W}{E}\right)^\tau f_B(\xi) + f_c \left(\frac{W}{E}\right)^m \left(1 - \frac{W}{E}\right)^6 \xi^\nu e^{-\gamma\xi}, \quad (27)$$

where f_B is the Born oscillator strength given by Eq. (24) and τ , m , δ , ν , γ , and f_c are parameters. On the basis of several phenomenological studies,^{16–19} we have chosen $\tau = 2$, $m = 2$, $\delta = 0.5$, $\nu = 1$, $\gamma = 0.17$, and $f_c = 0.1f_0$. These are not to be taken very seriously but simply as representative of the types of departures from Born approximation that might be expected. We note that this form of the DGOS preserves the analytic nature of the total cross section which goes over at high energies (e.g., above 500 eV) to the Born cross section.

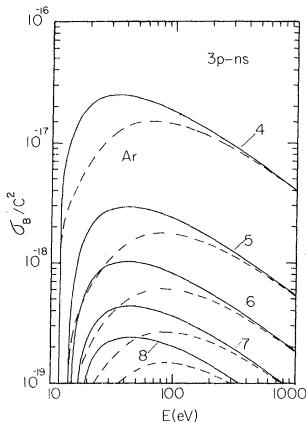


FIG. 11. Reduced cross sections for Argon (see caption to Fig. 10).

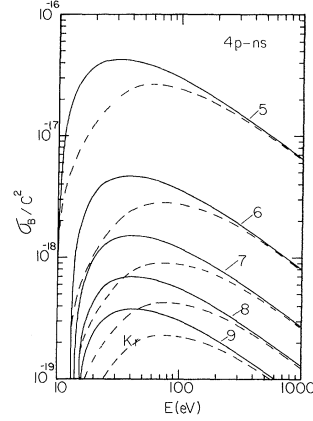


FIG. 12. Reduced cross sections for krypton (see caption to Fig. 10).

Figures 10–13 now define various $n_0 p$ - ns rare-gas cross sections apart from the constants C^2 . To arrive at these constants we avail ourselves of the fact that generalized oscillator strengths go over to the optical oscillator strengths as the momentum transfer goes to zero. Accordingly, if we know f_0 and Υ_0^2 , we can establish C^2 [see Eq. (26)]. In Sec. VIII we discuss optical oscillator strength data for $n_0 p$ - ns transitions in rare gases.

VIII. OPTICAL OSCILLATOR STRENGTHS

A compilation of reported experimental and theoretical optical oscillator strengths for the $n_0 p$ - $(n_0 + 1)s$ transition in rare gases adapted from Dow and Knox²⁰ is given in Table VI. The sources of data^{21–31} are indicated in column 2 and the references. It should be clear from the reported results that at this time theory and experiment still differ markedly. Since we do not attempt here to predict the relative strengths of the states within

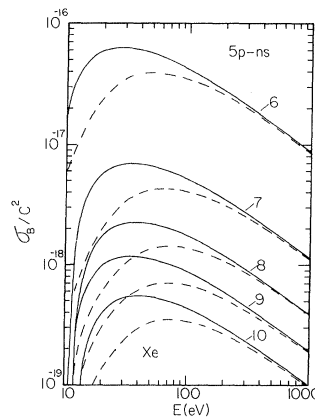


FIG. 13. Reduced cross sections for xenon (see caption to Fig. 10).

TABLE VI. Oscillator strengths for $n_0p-(n_0+1)s$ transitions in rare gases.

Atom	Ref.	1f	3f	f	f/Υ_0^2
Ne	21	0.110	0.011	0.121	1.32
	21	0.121	0.012	0.133	1.45
	22	0.163	1.78
0.0918 ^a	23	0.140	1.52
	24	0.130	0.008	0.138	1.50
	25	0.168	0.012	0.180	1.96
Ar	21	0.17	0.052	0.22	1.38
	21	0.200	0.049	0.25	1.56
	22	0.330	2.06
0.160 ^a	23	0.233	1.46
	26	0.228	0.059	0.287	1.79
	25	0.278	0.063	0.341	2.13
Kr	20	0.136	0.138	0.274	1.21
	20	0.153	0.152	0.305	1.35
	22	0.405	1.79
0.226 ^a	27	0.135	0.158	0.293	1.29
	28	0.266	0.266	0.346	1.53
	29	0.184	0.204	0.388	1.71
	23	0.346	1.53
	23	0.346	1.53
Xe	20	0.147	0.194	0.341	1.33
	20	0.170	0.190	0.360	1.40
	30	0.238	0.256	0.494	1.92
0.257 ^a	31	0.189	0.212	0.401	1.56
	25	0.238	0.256	0.494	1.92

^aDenotes Υ_0^2 for gas.

a multiplet, only the total strengths of the single-particle states will be considered. If we divide the composite strengths of the 3P and 1P terms by our calculated values of Υ_0^2 , we obtain the C^2 given in the last column of Table VI. We note that the variability of C^2 for each substance is quite comparable to the over-all variability. Accordingly it is not unreasonable to choose a single $C^2=1.5$ as a coefficient for translating our calculated Υ_0^2 into single-particle oscillator strengths.

While we only have very little information on other than resonance transitions, we can accept the $(n-\delta)^{-3}$ rule for single-particle oscillator strengths. We have examined this rule for $n_0p \rightarrow ns$ Rydberg series members in Ne and Ar and found that available oscillator strengths³² conform

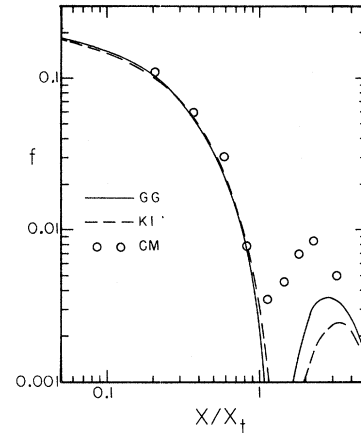


FIG. 14. Generalized oscillator strengths for "triplet" $5p-6s$ transition in xenon versus x/x_t . The circles denote experimental data, the dashed curve a Hartree-Fock calculation, and the solid curve our IPM calculation.

quite well to this law with quantum defect given in Table IV. Accordingly it is reasonable to infer all single-particle oscillator strengths by using Eq. (19) with C^2 given by 1.5 and Υ_0^{*2} as in Table IV.

No simple rule can be given for decomposing these strengths into their multiplet components since the coupling scheme varies from gas to gas and state to state. Thus to obtain such a breakdown one will have to lean upon detailed spectroscopic assignment of the optical strengths. Such numbers are becoming available.

While we have examined a number of recent extensive studies of electron impact excitation of atoms,³³⁻³⁵ we have found very few direct experimental data on rare gases to test the detailed aspects of our generalized oscillator strengths or excitation cross sections. Chamberlain and Mielczarek (CM) at the National Bureau of Standards³¹ have reported generalized oscillator strengths for the $5p-6s$ "triplet" transition in Xe which display a minimum at about $\xi=1$. Figure 14 shows their data, the results of a theoretical calculation of Kim and Inokuti (KI) using HF wave functions,³¹ and the results of our IPM adjusted to the same optical oscillator strength (0.212). The two calculations are in reasonable agreement and

TABLE VII. Parameters for n_0p-nd analytic generalized oscillator [use $\Upsilon_{0n} = \Upsilon_0^*/(n-\delta)^{3/2}$].

	$m=0$					$m=1$				
	Υ_0^*	δ	α_0	χ	α_1	Υ_0^*	δ	α_0	χ	α_1
Ne	-0.780	-1.23	2.60	0.036	0.33	0.64	-1.11	1.25	-0.10	0.45
Ar	-2.81	-0.44	1.55	0.020	0.17	-2.39	-0.39	0.85	-0.10	0.36
Kr	-2.21	1.51	1.55	0.080	0.37	-1.93	1.57	1.00	-0.14	0.50
Xe	-1.39	3.51	2.35	0.24	0.55	-1.33	3.53	1.25	-0.30	0.70

in reasonable conformity with experiment. The fact that the experimental peak beyond the first minimum lies above the calculated IPM and HF values is probably an indication of a breakdown of the Born approximation.

We have also carried out calculations of $n_0 p$ - nd transitions for four members of Rydberg series for each of the rare gases. Here graphs of the $m=0$ transitions based upon III(a) in Table III show an over-all behavior which is, roughly speaking, similar to that in Figs. 5-8. However, the $m=1$ transitions based upon III(b) in Table III have fewer nodes and are much smoother in shape. In Table VII we give parameters for the relationship $T_{0n} = T_{0n}^*/(n-\delta)^{3/2}$ and for Eq. (20) which characterize the generalized oscillator strengths for the $n_0 p$ - nd Rydberg series out to $\xi \sim 20$. Here one sees a major advantage of the approximate analytic representation since it would take eight figures each with four curves to convey much less precisely the useful aspects of our calculations. Again our work indicates that scaling by ξ is quite good within the second node. Identification of the optical oscillator strengths and application of the cross sections to electron energy deposition in argon is underway in a separate study.³⁶

IX. SUMMARY AND CONCLUSION

The primary purpose of this work has been to apply a realistic IPM¹ to the programmatic generation of generalized oscillator strengths. The fact that it is possible to do this permits us to bypass present obstacles due to the lack of HF excited-state wave functions. Our work is also intended to lay the groundwork for distorted-wave-approximation calculations, of inelastic collisions.³⁶ In such calculations consideration is given to exchange effects and the distortion of the incoming wave and outgoing wave by the potential presented by the neutral atom. Such work will provide a basis for low-energy cross-section assignments and for direct comparison with experimental data.

The approximate analytic representations for the generalized oscillator strength which we have found

should be useful as a compact way of inputting specific cross sections into such applied calculations as electron-energy deposition problems.³⁷⁻³⁹ We believe it should be possible to extend the analytic representation of the generalized oscillator strength into the low-energy region and such work is under way.

We might note here that we have also calculated generalized oscillator strengths for $n_0 p_0$ - np forbidden transitions. These are found to vanish at $\xi=0$ as might have been expected from the orthogonality of the radial wave functions in a common central potential which includes the centrifugal energy. This natural property of an IPM potential is another advantage with respect to the use of Hartree-Fock excited-state wave functions, apart from the fact that very few of the latter are available. We also have under way calculations of continuous generalized oscillator strengths.⁴⁰ As might be expected, their properties are reasonable extrapolations of the upper members of the Rydberg series which we have calculated here.

Perhaps our most important result is the clear demonstration of systematic behavior in generalized oscillator strengths for Rydberg series in rare-gas atoms. Scaling by the use of the variable $\xi = K^2 a_0^2 R/W$ seems to be a useful way of correlating generalized oscillator strengths out to the second node. While Kim *et al.*³¹ have previously noted the existence of the first minima in generalized oscillator strengths, the fact that generalized oscillator strengths have a complex nodal structure at large values of K^2 seems not to have been noted. This feature will be further elucidated in distorted-wave calculations of generalized oscillator strengths.⁴¹

ACKNOWLEDGMENTS

The authors would like to thank Dr. J. E. Purcell, Dr. T. Sawada, Dr. L. R. Peterson, and R. A. Berg for helpful discussions and A. Yezzi, J. Londono, and C. Pittman for help with the calculations and the drawings.

*Work supported by the U. S. Atomic Energy Commission.

[†]Present address: California State College at Los Angeles, Los Angeles, Calif. 90032.

¹A. E. S. Green, D. L. Sellin, and A. S. Zachor, *Phys. Rev.* **184**, 1 (1969).

²J. E. Purcell, R. A. Berg, and A. E. S. Green, *Phys. Rev. A* **2**, 107 (1970).

³R. A. Berg, J. E. Purcell, and A. E. S. Green, *Phys. Rev. A* **3**, 509 (1971).

⁴A. E. S. Green, D. L. Sellin, and G. Darewych, *Phys. Rev. A* **3**, 159 (1971).

⁵J. W. Darewych, A. E. S. Green, and D. L. Sellin, *Phys. Rev. A* **3**, 502 (1971).

⁶K. Siegbahn *et al.*, *ESCA Atomic Molecular and Solid*

State Structure Studied by Means of Electron Spectroscopy (Almqvist & Wiksells Boktryckeri AB, Uppsala, Sweden, 1967).

⁷J. B. Mann, Los Alamos Scientific Laboratory, Report No. LA-3690, 1968 (unpublished).

⁸F. Herman and S. Skillman, *Atomic Structure Calculations* (Prentice-Hall, Englewood Cliffs, N. J., 1963).

⁹C. E. Moore, *Atomic Energy Levels*, Natl. Bur. Std. (U. S.) Circ. No. 467 (U. S. GPO, Washington, D. C., 1958), Vols. I-III.

¹⁰H. Bethe, *Ann. Phys. (Leipzig)* **5**, 325 (1930).

¹¹N. F. Mott and H. S. W. Massey, *The Theory of Atomic Collisions* (Clarendon, London, 1965).

¹²A. E. S. Green and S. K. Dutta, *J. Geophys. Res.*

72, 3933 (1967).

- ¹³R. A. Bonham, *J. Chem. Phys.* **36**, 3260 (1962).
¹⁴U. Fano and J. W. Cooper, *Phys. Rev.* **137**, A1364 (1965).
¹⁵W. Gautschi and W. F. Cahill, in *Handbook of Mathematical Functions*, edited by M. Abramowitz and I. A. Stegun (U. S. GPO, Washington, D. C., 1964), Appl. Math. Series 55, Chap. 5.
¹⁶A. T. Jusick, C. E. Watson, L. R. Peterson, and A. E. S. Green, *J. Geophys. Res.* **72**, 3943 (1967).
¹⁷R. S. Stolarski, V. A. Dulock, C. E. Watson, and A. E. S. Green, *J. Geophys. Res.* **72**, 3953 (1967).
¹⁸C. E. Watson, V. A. Dulock, R. S. Stolarski, and A. E. S. Green, *J. Geophys. Res.* **72**, 3961 (1967).
¹⁹D. J. Strickland and A. E. S. Green, *J. Geophys. Res.* **74**, No. 26 (1969).
²⁰J. D. Dow and R. S. Knox, *Phys. Rev.* **152**, 50 (1966).
²¹A. Gold and R. S. Knox, *Phys. Rev.* **113**, 834 (1959).
²²J. W. Cooper, *Phys. Rev.* **128**, 681 (1962).
²³J. Geiger, *Z. Physik* **177**, 138 (1964).
²⁴G. M. Lawrence and H. S. Liszt, *Phys. Rev.* **178**, 122 (1969).
²⁵E. L. Lewis, *Proc. Phys. Soc. (London)* **92**, 817 (1967).
²⁶G. M. Lawrence, *Phys. Rev.* **175**, 40 (1968).

- ²⁷P. G. Wilkinson, *J. Quant. Spectry. Radiative Transfer* **5**, 503 (1965).
²⁸J. Koch, *Kgl. Fysiograf. Sallskap. Lund Forh.* **19**, 173 (1949).
²⁹J. M. Vaughan, *Phys. Rev.* **166**, 13 (1968).
³⁰D. K. Anderson, *Phys. Rev.* **137**, A21 (1965).
³¹Y. K. Kim, M. Inokuti, G. E. Chamberlain, and S. R. Mielczarek, *Phys. Rev. Letters* **21**, 1146 (1968).
³²C. E. Kuyatt (private communication).
³³L. A. Vainshtein and I. I. Sobel'man, *J. Quant. Spectry. Radiative Transfer* **8**, 1491 (1968).
³⁴V. Ya. Veldre, A. V. Lyash, and L. L. Rabik, *Opt. Spectry. (USSR)* **19**, 182 (1965).
³⁵B. L. Moiseiwitsch and S. J. Smith, *Rev. Mod. Phys.* **40**, 238 (1968).
³⁶T. Sawada, J. E. Purcell, and A. E. S. Green, following paper, *Phys. Rev. A* **4**, 192 (1971).
³⁷R. S. Stolarski and A. E. S. Green, *J. Geophys. Res.* **72**, 3967 (1967).
³⁸A. E. S. Green and C. A. Barth, *J. Geophys. Res.* **72**, 3974 (1967).
³⁹L. R. Peterson and A. E. S. Green, *J. Phys. B* **1**, 1131 (1968).
⁴⁰R. A. Berg and A. E. S. Green (unpublished).
⁴¹L. R. Peterson and J. E. Allen, Jr. (unpublished).

Distorted-Wave Calculation of Electron Impact Excitation of the Rare Gases*

T. Sawada, J. E. Purcell,[†] and A. E. S. Green
University of Florida, Gainesville, Florida 32601
 (Received 11 January 1971)

A distorted-wave (DW) formulation with exchange is given for the electron impact excitation of the rare gases from $(n_0p)^6$ to $(n_0p)^5nl$ configurations. A practical form employing the pure LS -coupling scheme is used in conjunction with the phenomenologically determined independent-particle model (IPM) and the DW potentials of real central forms to compute cross sections averaged over fine structures. Numerical work is carried out for Ne $2p \rightarrow 3s$ and Ar $3p \rightarrow 4s$ electron impact excitations. The distorted generalized oscillator strengths (DGOS), which converge to the generalized oscillator strengths (GOS) in the limit of the Born approximation, as well as integrated cross sections, are obtained over a wide range of energies, so that the systematic variation of the cross sections in relation to the results of the Born approximation can be studied. The results of the angular distributions at lower energies are in reasonable agreement with the data by Nicoll and Mohr.

I. INTRODUCTION

The electron impact excitation of the rare gases has been studied in the Born approximation by Ganas and Green, based upon the analytic atomic IPM of Green, Sellin, and Zachor.^{1,2} In order to extend their work to lower-energy regions, it is necessary to investigate the effects of distortion as well as exchange contributions. We study these effects using the DW approximation based upon the same IPM² and the same DW potential that has been applied to the elastic scattering analysis.³

Very few DW calculations have been reported for atoms heavier than hydrogen and helium, with the

exception of the work by Massey and Mohr on the low-energy data of Ne and Ar obtained by Nicoll and Mohr.^{4,5} If the excitation cross sections of individual levels in a fine structure were required, one would have to first obtain Hartree-Fock (HF) atomic wave functions and HF potentials of the initial and final states. A detailed DW formulation appropriate for such a computation has been proposed recently by Shelton and Leherissey⁶ with particular emphasis on a transition from the LS -coupled ground state to a J_Ol -coupled excited state.

In this work, however, we are interested primarily in obtaining cross sections averaged over an energy interval whose width is of the order of